Editors' Suggestion

Percolation and Topological Properties of Temporal Higher-Order Networks

Leonardo Di Gaetano,[1] Federico Battiston,[1,*] and Michele Starnini[2,3,†]
[1]Department of Network and Data Science, Central European University, 1100 Vienna, Austria
[2]Departament de Fisica, Universitat Politecnica de Catalunya, Campus Nord, 08034 Barcelona, Spain
[3]CENTAI Institute, 10138 Turin, Italy

(Received 1 June 2023; revised 23 October 2023; accepted 11 December 2023; published 18 January 2024)

Many complex systems that exhibit temporal nonpairwise interactions can be represented by means of generative higher-order network models. Here, we propose a hidden variable formalism to analytically characterize a general class of higher-order network models. We apply our framework to a temporal higher-order activity-driven model, providing analytical expressions for the main topological properties of the time-integrated hypergraphs, depending on the integration time and the activity distributions characterizing the model. Furthermore, we provide analytical estimates for the percolation times of general classes of uncorrelated and correlated hypergraphs. Finally, we quantify the extent to which the percolation time of empirical social interactions is underestimated when their higher-order nature is neglected.

DOI: 10.1103/PhysRevLett.132.037401

An extremely broad category of complex systems can be represented as networks, where nodes describe units and links encode their pairwise interactions [1]. Despite widespread use, the dyadic structure does not allow for an accurate description of all those systems where nonpairwise interactions play a fundamental role, from human [2] and animal [3] social networks to collaboration networks [4], drug recombination [5], cellular networks [6], species interactions [7], and the human brain [8–10]. Such systems are better described by hypergraphs [11], where hyperedges encode interactions among an arbitrary number of system units [12]. Taking into account higher-order interactions has been shown to significantly affect collective behaviors in networked dynamics [12,13], including diffusion [14,15], synchronization [16–21], contagion [22–24], and evolutionary [25–27] processes.

Furthermore, networks are inherently dynamic, with interactions evolving in time [28]. While extensive research has been devoted to model temporal networks [29–31] and the behavior of dynamical processes unfolding on their top [32–35], the interest in temporal higher-order networks blossomed only recently. Higher-order interactions have been observed to occur in bursts in real face-to-face interaction systems [36] and display temporal correlations among different orders [37], and temporal dynamics is known to affect the epidemic threshold in higher-order models of social contagion [23,38]. With a few notable exceptions [37,39], most models of higher-order networks are static generalizations of Erdos-Renyi [40] or configuration models [41–43] or are limited to networks that grow over time [44,45]. Modeling temporal group dynamics and predicting their connectivity properties at the microscale is still an open problem.

Here, we introduce a general approach to analytically characterize higher-order time-varying networks by means of a hidden variable (HV) framework. In pairwise networks, HVs were introduced to model the presence of links in networks with structural correlations [46]. Until now, the HV formalism has been employed across a vast spectrum of first-order generative processes, such as to map networks into embedded spaces, including latent [47] and hyperbolic spaces [48], fitness models [49,50], protein interaction [51], and social distance [52]. Furthermore, the HV formalism has been applied to networks evolving over time [53] and networks with inherent correlations [46], and subsequently employed to pinpoint the topological characteristics of activity-driven networks [31,54,55]. However, the aforementioned works neglected the higher-order organization of the considered social and biological systems.

In this Letter, we propose a higher-order HV formalism that provides a powerful approach to describe higher-order networked systems, applicable to a wide range of generative models. As a demonstration of its versatile applicability, we apply our framework to a higher-order activity-driven model, where group interactions of different sizes are generated over time. We study the connectivity properties of the time-integrated system, obtaining analytical asymptotic expressions for the hyperdegree distribution and hyperdegree correlations over time. We obtain these results in the limit of sparse networks and large hyperdegrees. We provide analytical estimates for the percolation times of general classes of uncorrelated and correlated hypergraphs marking the onset of a giant connected component in the higher-order systems. We conclude by showing that neglecting the higher-order nature of interactions in empirical social networks leads to systematically

underestimating the percolation threshold, with implications for any dynamical process running on such systems.

Higher-order hidden-variable formalism.—We start by developing the HV formalism for higher-order networks. Each node i of a network of N nodes is endowed with an intrinsic vectorial HV $\mathbf{h}_i = (h_i^{(1)}, h_i^{(2)}, \ldots, h_i^{(m)}, \ldots)$, where the HV $h_i^{(m)}$ determines the m-order interactions of node i. For each order m, $h_i^{(m)}$ is drawn from an independent distribution $\rho(h^{(m)})$. The higher-order HV model assumes that the existence of an m-order hyperlink among $m+1$ nodes depends only on their HV, i.e., a connection probability $\mathrm{IP}(h_1^{(m)}, \ldots, h_m^{(m)}, h_{m+1}^{(m)})$. In general terms, the hyperdegree distribution $P(k^{(m)})$ (being $k^{(m)}$ the number of m-links of a node) can be written as a function of the HV distribution as

$$P(k^{(m)}) = \sum_{h^{(m)}} g(k^{(m)}|h^{(m)})\rho(h^{(m)}), \tag{1}$$

where $g(k^{(m)}|h^{(m)})$ is the conditional probability (propagator) that a node with HV $h^{(m)}$ ends up with a certain hyperdegree $k^{(m)}$.

As in the first-order case [46], the propagator can be expressed as the convolution of partial propagators. For instance, for $m = 2$,

$$g(k^{(2)}|h^{(2)}) = \sum_{\{k_{ij}^{(2)}\}} \delta^{k^{(2)}}_{\sum k_{ij}^{(2)}} \prod_{i\geq j}^{C} g_{ij}^{(h^{(2)})}(k_{ij}^{(2)}|h_i^{(2)}, h_j^{(2)}), \tag{2}$$

where $g_{ij}^{(h^{(2)})}(k_{ij}^{(2)}|h_i^{(2)}, h_j^{(2)})$ is the probability that a node (with HV $h^{(2)}$) ends up with $k_{ij}^{(2)}$ second-order interactions, with neighbors of HVs $h_i^{(2)}$ and $h_j^{(2)}$. In the convolution, we take into account all the possible pairs of classes of HVs excluding permutations ($i \geq j$), being $h_C^{(2)}$ the maximum value of $h^{(2)}$, and we sum over the set of all possible second-order degree values $\{k_{ij}^{(2)}\} = \{k_{11}^{(2)}, k_{12}^{(2)}, \ldots, k_{CC}^{(2)}\}$. The Kronecker delta constrains that the final second-order degree $k^{(2)}$ is equal to the sum of the partial degrees $k_{ij}^{(2)}$. See Supplemental Material [56] for the explicit m-order general expression.

For any m, one can solve the convolutional equation by resorting to the generating function of the propagator, $\hat{g}(z|h^{(m)}) = \sum_k z^{k^{(m)}} g(k^{(m)}|h^{(m)})$, where, for a lighter notation, from now on we indicate $h^{(m)}$ as h. Since the propagator is the convolution of partial propagators, given by Eq. (2), its generating function is equal to the product of the generating functions of the partial propagators. If hyperlinks are independently drawn according to the HV of nodes, the partial propagators are binomial distributions, and their generating functions can be obtained easily (see [56]). The logarithm of the generating function can be eventually written as a function of the HV distribution and the connection probability $\mathrm{IP}(h, h_1, \ldots, h_m)$,

$$\ln[\hat{g}(z|h)] = \frac{N^m}{m!} \sum_{h_1,\ldots,h_m} \rho(h_1), \ldots, \rho(h_m), \times \ln\left[1 - (1-z)\mathrm{IP}(h, h_1, \ldots, h_m)\right], \tag{3}$$

where one has to sum (integrate) over m HV distributions and the factor $m!$ comes from excluding permutations.

In the limit of sparse networks, $\mathrm{IP}(h, h_1, \ldots, h_m) \ll 1$, the generating function of the propagator is exponential, thus indicating that the propagator is a Poisson distribution for every order m, as in the dyadic case $m = 1$ [46]. From the generating function of the propagator $\hat{g}$, one can compute the expected m degree of a node with HV h by means of the first derivative of $\hat{g}(z|h)$ at $z = 1$ [46], and it reads

$$\bar{k}^{(m)}(h) = \frac{N^m}{m!} \sum_{h_1,\ldots,h_m} \rho(h_1), \ldots, \rho(h_m)\mathrm{IP}(h, h_1, \ldots, h_m). \tag{4}$$

Instead, the problem-specific piece of information that allows us to treat different models is contained in Eq. (4) through the connection probability $\mathrm{IP}(h, h_1, \ldots, h_m)$, which is the key ingredient to find the hyperdegree distribution, given by Eq. (1).

Similarly, we can study hyperdegree correlations starting from the conditional connection probability. We define the average m-order degree of the neighbors of a node with HV h as (see Supplemental Material [56]),

$$\bar{k}_{nn}^{(m)}(h) = \sum_{h_1,\ldots,h_m} \left(\frac{\bar{k}^{(m)}(h_1) + \cdots + \bar{k}^{(m)}(h_m)}{m}\right) p(h_1, \ldots, h_m|h), \tag{5}$$

where $p(h_1, \ldots, h_m|h)$ is the conditional probability that a node with HV h is connected to nodes with HV $h_1, h_2, \ldots, h_m$. The average m degree of the neighbors of a node with m degree k, $\bar{k}_{nn}^{(m)}(k)$, can be eventually found by following [46], obtaining a form equivalent to the first-order case. Therefore, the HV formalism allows us to obtain the hyperdegree correlations of a large variety of higher-order generating processes simply by knowing the HV distribution and the connection probability depending on these variables.

The higher-order activity-driven model.—We apply the higher-order HV framework to the higher-order activity-driven (HOAD) model, describing temporal group dynamics, inspired by a very similar model for simplicial complexes [39]. Each agent i in a population of size N

is endowed with a higher-order activity potential $\mathbf{a}_i = (a_i^{(1)}, a_i^{(2)}, \ldots, a_i^{(m)})$ for every interaction order m. The activities of the agents are random variables, extracted from distributions $\rho(\mathbf{a}) = (\rho(a^{(1)}), \rho(a^{(2)}), \ldots, \rho(a^{(m)}))$, which we assume to be independent. The activity of node i at order m, $a_i^{(m)}$, represents the probability that they engage in an interaction with m other nodes in a certain time interval Δt.

The HOAD model generates temporal hypergraphs starting by N initially disconnected nodes. At every time step, each node i generates one hyperlink of order m toward randomly selected nodes, with probability proportional to their activity $a_i^{(m)}$. At the following time step, the existent higher-order interactions are erased and the process continues. The temporal hypergraph is defined by the sequence of instantaneous, sparse hypergraphs generated at each time step. One can obtain a static hypergraph by integrating all instantaneous hypergraphs up to a certain time T, where two nodes i and j will be connected if any hyperedge between them exists in any instantaneous hypergraph in $t \in [1, T]$.

Topological properties of HOAD networks.—We now compute the topological properties of the HOAD networks integrated up to a certain time T by mapping the HOAD model to the HV formalism. First, since the activity distributions of different orders are assumed independent, we treat every order separately and omit the order dependency for brevity from now on, $a = a^{(m)}$. The key step for the HV mapping resides in computing the probability that a node with activity potential a_i will be connected with a set of m other nodes, with activity $a_1, \ldots, a_m$, at time T in the integrated network, namely, $\mathrm{IP}_T(a, a_1, \ldots, a_m)$. By following [54], we can find this expression starting from the probability $\mathcal{Q}_T(a, a_1, \ldots, a_m) = 1 - \mathrm{IP}_T(a, a_1, \ldots, a_m)$ that the set of $m+1$ nodes is not connected by an m-order link until time T. Considering that every time a node is active it selects m random neighbors for an m-order link and that the number of times a node can be active until time T is described by a binomial distribution, we write

$$\mathrm{IP}_T(a, a_1, \ldots, a_m) \simeq \frac{m!}{N^m}(a + a_1 + \cdots + a_m)T, \quad (6)$$

where we have worked in the limit of $N \gg T \gg 1$ (see Supplemental Material [56]). By inserting Eq. (6) into Eq. (4), we can obtain for $N \gg m$ the expected m-order degree of nodes with activity a, at time T,

$$\bar{k}_T^{(m)}(a) \simeq T(a + m\langle a \rangle), \quad (7)$$

where $\langle a \rangle = \sum_a a\rho(a)$ denotes the usual average of activity of order m over the population. The expected m-order degree is intuitively equal to aT outgoing m-order links plus $mT\langle a \rangle$ connections received from random neighbors.

By inserting Eq. (7) into the Poissonian form of the propagator and substituting it into Eq. (1), one can obtain the asymptotic limit of the degree distribution of order m of the aggregated network until time T (see Supplemental Material [56]),

$$P_T(k^{(m)}) \simeq \frac{1}{T}\rho\left(\frac{k^{(m)}}{T} - m\langle a \rangle\right). \quad (8)$$

The last expression is obtained in the limit of large N and small T, $T \ll (N^m/m!)$ and for $T^2 \gg k^{(m)} \gg 1$ (see Supplemental Material [56]). Figure 1(a) shows the hyperdegree distribution $P_T(k^{(m)})$ of HOAD networks integrated at time T, as obtained by numerical simulations. We arbitrarily select a power-law activity distribution, yet Eq. (8) is general for any distribution ρ. The model is implemented as part of the library HGX [57]. One can see

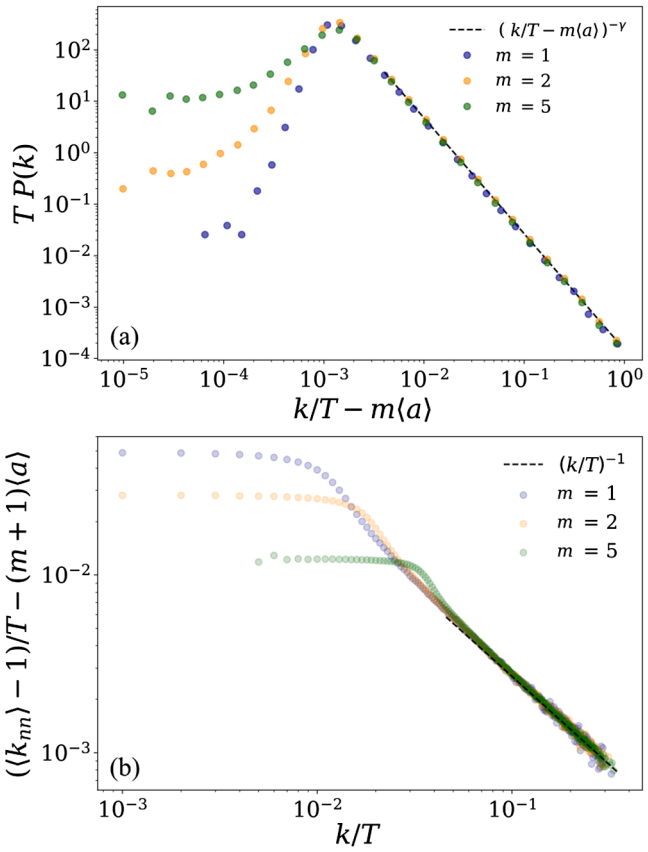

FIG. 1. Topological properties of HOAD networks. (a) Hyperdegree distribution $P_T(k^{(m)})$; Eq. (8) shown as a dashed line. (b) Hyperdegree correlations $\bar{k}_{nn,T}^{(m)}(k)$; Eq. (9) shown as a dashed line. Network size $N = 10^6$, orders $m = 1, 2, 5$, integration time $T = 10^3$. Different values of T and m are shown in the Supplemental Material [56]. The activity distributions $\rho(a)$ of order m have a power-law form for every order with exponent $\gamma = 2.25$.

a good agreement with the asymptotic behavior indicated by Eq. (8).

Hyperdegree correlations of HOAD networks.—The average m-order degree of the neighbors of a node with activity a at time T, $\bar{k}^{(m)}_{nn,T}(a)$, is obtained by the HV mapping of Eq. (5). To this aim, one needs to compute the conditional probability $p(a_1, a_2, \ldots, a_m|a)$ that a node with activity a is connected to nodes with activities $a_1, a_2, \ldots, a_m$ by using the connection probability of the HOAD model, given by Eq. (6), and the expected m degree of nodes with activity a at time T, given by Eq. (7). After obtaining $\bar{k}^{(m)}_{nn,T}(a)$ (see Supplemental Material [56] for the analytical expression), the m-order degree-degree correlation can be obtained by following [46] and it reads

$$\frac{\bar{k}^{(m)}_{nn,T}(k) - 1}{T} \simeq (m+1)\langle a\rangle + \sigma^2 \left(\frac{k^{(m)}}{T}\right)^{-1}, \tag{9}$$

where $\sigma^2 = \langle a^2\rangle - \langle a\rangle^2$ of the m-order activity.

The last expression, valid in the limit of $k^{(m)} \gg 1$ and sparse network (Supplemental Material [56]), gives an asymptotic prediction of $\bar{k}^{(m)}_{nn,T}(k)$ as a function of the first two momenta of the activity distribution of order m. Figure 1(b) shows the correlations minus its first moment of HOAD networks integrated at time T, as obtained by numerical simulations. As for the degree distribution, we plot the rescaled hyperdegree correlations, the differences between the correlations and their leading approximation in order to show how it decays with $T/k^{(m)}$ and the collapse of the curves for three different orders $m = 1, 2, 5$. One can see that the disassortative behavior proportional to $(k^{(m)})^{-1}$ and governed by σ^2, as predicted by Eq. (9), is confirmed by numerical simulations.

Temporal percolation of HOAD networks.—The connectivity properties of the time-integrated HOAD networks allow us to characterize the temporal percolation, i.e., the time T_p marking the onset of a giant connected component in the integrated network. The percolation time T_p is particularly relevant for dynamical processes unfolding of these temporal networks, since any process with a characteristic lifetime smaller than T_p will be unable to explore a sizable fraction of the network.

The details of the derivation of the percolation times are reported in the Appendix. We first obtain the conditions for the percolation threshold of static correlated and uncorrelated hypergraphs of order m. Then, we map these results into the HOAD model, by writing the degree momenta as a function of the activity distribution, thus finding the percolation times for correlated and uncorrelated HOAD networks. The percolation time for correlated HOAD networks of order m reads

$$T_c^{(m)} = \frac{2}{\langle a\rangle(m+1) + \sqrt{\langle a\rangle^2(m^2+2m-3) + 4\langle a^2\rangle}}. \tag{10}$$

We test the validity of the prediction given by Eq. (10) by running extensive numerical simulations. Figure 2(a) shows the growth of the giant component size S over time and the peak of its variance $\sigma(S)^2$, indicating the estimated percolation time, for several orders m. The percolation time predicted by Eq. (10) has a decent agreement with numerical results, yet they do not exactly coincide. We thus run a finite-size scaling analysis by assuming that the relative difference between the actual percolation time $T_c^{(m)}$ in the thermodynamic limit and the one found in a network of size N, $T^{(m)}(N)$, follows a scaling law of the form $[T^{(m)}(N) - T_c^{(m)}]/T_c^{(m)} \sim N^{-\nu}$ for every m. Figure 2(b) shows that the finite-size hypothesis holds; the percolation time estimated by the peak over time of the variance of the

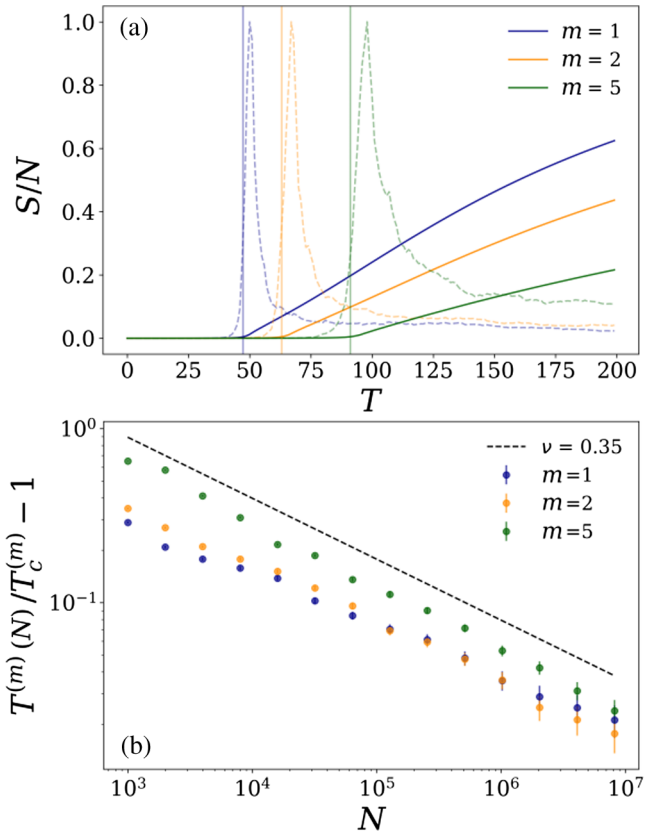

FIG. 2. Percolation time of HOAD networks. Orders $m = 1, 2, 5$. (a) Giant component size S/N (continuous line) and the peak of its variance $\sigma(S)^2$ (dashed line) over time. The theoretical prediction given by Eq. (10) is indicated as a vertical line. (b) Finite-size scaling analysis of the relative difference $[T^{(m)}(N) - T_c^{(m)}]/T_c^{(m)}$ (circles) and corresponding scaling law $N^{-\nu}$ (dashed line). Results are averaged over 10^2 runs.

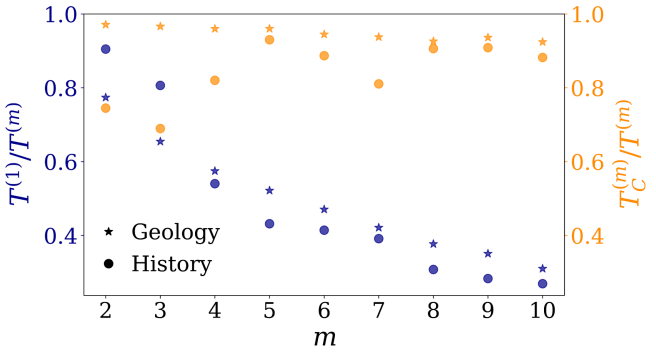

FIG. 3. Percolation times in empirical data. Geology (stars) and history (circles) scientific collaboration networks. Blue points, ratios between the first-order ($T^{(1)}$) and m-order ($T^{(m)}$) percolation times of networks informed by empirical activities, estimated from numerical simulations; yellow points, ratios between the theoretical prediction from Eq. (10) $T_c^{(m)}$ and the percolation times of networks informed by empirical activities estimated from numerical simulations $T^{(m)}$.

giant component size actually approaches $T_c^{(m)}$ for any order m in the thermodynamic limit $N \to \infty$.

Empirical data.—Finally, we show the potential of the HOAD modeling framework by testing the theoretical predictions for the percolation time on higher-order empirical data, comparing it with the first-order percolation. For this latter case, we project all interactions into the first order, thus representing higher-order data as a simple network, losing part of the information contained therein. We consider two datasets of scientific collaboration networks in the fields of geology and history, collected by the Microsoft Academic graph (see Supplemental Material [56] for details). We inform first- and higher-order activity-driven models with empirical activities extracted from the dataset and compare the first-order ($T^{(1)}$) and m-order ($T^{(m)}$) percolation times of the networks. The percolation points are obtained by calculating the time for which the variance of the component size distribution is maximum.

Figure 3 shows that the m-order percolation time $T^{(m)}$ estimated by numerical simulations of the HOAD model informed by empirical data is in good agreement with the theoretical prediction $T_c^{(m)}$ given by Eq. (10) for every order m. Moreover, Fig. 3 shows that the first-order percolation time $T^{(1)}$ is much smaller than the actual m-order one $T^{(m)}$ and such a difference increases with the order m. Therefore, an incorrect representation of higher-order data as classic dyadic interactions leads to a substantial underestimation of the true higher-order percolation times, up to 50% already for $m = 5$; that is, small groups of six people.

Conclusions.—In this Letter, we showed that the topological and percolation properties of temporal higher-order networks can be obtained by mapping such networks to a higher-order HV formalism. We illustrate the potential of our theoretical framework by quantitatively showing how much the percolation times of higher-order empirical social networks are underestimated if higher-order interactions are neglected. This result is particularly interesting within the framework of epidemic processes: a disease spreading with a short timescale is expected to percolate when the underlying contact network is assumed to be formed by dyadic interactions, but it would not percolate in the corresponding higher-order network representation. Note, however, that our finding holds within the specific activity-driven modeling framework. Further research should be devoted to addressing this setting in different modeling frameworks and on real contact networks.

The higher-order HV framework we developed holds potential for future applications across a wide array of higher-order and temporal generative models. For instance, it could be applied to higher-order fitness models [49] or social dynamics models including higher-order interactions mapped into latent spaces [52]. Likewise, it could be extended to describe network models incorporating non-Markovian dynamics [31], which has shown to have a deep impact on epidemic processes. Future research could quantify and model the presence of correlations between different interaction orders, as well as their effects on the connectivity and percolation properties of time-integrated networks. We hope that our work will stimulate further research to apply the higher-order HV framework to other empirical, time-varying complex systems.

We acknowledge Romualdo Pastor-Satorras for useful discussions. F. B. acknowledges support from the Air Force Office of Scientific Research under Grant No. FA8655-22-1-7025.

Appendix: Temporal percolation.—Here we show how we calculate the percolation times for correlated and uncorrelated HOAD networks. We first consider static hypergraphs of order m whose nodes may be removed with probability $1 - p$. Following the approach outlined in [58], we determine the probability x_k of avoiding a giant connected component while traversing an m-order hyperlink (connecting $m + 1$ nodes) starting from a node with hyperdegree k (we omit the dependency in m). This condition can be expressed as

$$x_k = \left[1 - p + p\sum_{k'} P(k'|k) x_{k'}^{k'-1}\right]^m, \tag{A1}$$

where $P(k'|k)$ is the probability that a node with m degree k is connected with a node of m-order degree k' and we assume that the probability $x_{k'}$ of each of the m nodes to be connected to the giant component is independent of each other, so we exponentiate the same probability to the m. Close to the percolation threshold, we have $x_k \lessapprox 1$; hence defining $y_k = 1 - x_k \gtrapprox 0$ and expanding Eq. (A1) (see Supplemental Material [56] for

detailed calculations), we get

$$y_k = mp\sum_{k'} \mathbf{B}^{(m)}_{kk'} y_{k'}, \tag{A2}$$

where we have defined the m-order branching matrix as $\sum_{k'} \mathbf{B}^{(m)}_{kk'} y_{k'} = \sum_{k'} (k'-1) P(k'|k) y_{k'}$. In addition to a multiplicative factor m, Eq. (A2) is equivalent to the result found for simple networks [58], having also the same elementwise representation of $\mathbf{B}^{(m)}_{kk'}$ for every m (see [56]). The last expression also allows us to find the percolation condition for uncorrelated hypergraphs, by writing the conditional probability as $P(k'|k) = \rho(k')k'/\langle k \rangle$. In this way, we find the m-order version of the well-known Molloy-Reed criterion [59] $\langle k^2 \rangle - \langle k \rangle / \langle k \rangle > 1/m$, already found in [60]. By explicitly writing the degree momenta as a function of the activity distribution, the percolation time for uncorrelated hypergraphs reads

$$T^{(m)}_{\mathrm{unc}} = \frac{(m+1)\langle a \rangle}{m(m+2)\langle a \rangle^2 + \langle a^2 \rangle}. \tag{A3}$$

The percolation threshold for correlated networks is instead given by the condition $m p_c \lambda^{(m)}_1 = 1$ from Eq. (A2), where $\lambda^{(m)}_1$ is the dominant eigenvalue of the m-order branching matrix $\mathbf{B}^{(m)}_{kk'}$, as guaranteed by the Perron-Frobenius theorem [58], and p_c is the critical density of nodes for the onset of a giant connected component. The largest eigenvalue $\lambda^{(m)}_1$ can be found by means of the HV formalism by following [55], as a function of the first and second degree momenta of order m, $\langle k \rangle_{T_p}$ and $\langle k^2 \rangle_{T_p}$ (see Supplemental Material [56]). We then map these expressions into the HOAD model, where the degree momenta are given by the activity distributions, and find the percolation time for correlated HOAD networks [Eq. (10) of the main text].

Both analytical predictions for correlated and uncorrelated networks depend on the first two momenta of $\rho(a)$. For large m, we have $T^{(m)}_{c,\mathrm{unc}} \propto (1/m) \to 0$ for both correlated and uncorrelated cases, so the uncorrelated percolation time approaches the correlated one in this limit. The difference between the two times is maximum for strongly heterogeneous networks, see the Supplemental Material [56].

*battistonf@ceu.edu
†michele.starnini@gmail.com

[1] S. Boccaletti, V. Latora, Y. Moreno, M. Chavez, and D.-U. Hwang, Phys. Rep. **424**, 175 (2006).
[2] A. R. Benson, R. Abebe, M. T. Schaub, A. Jadbabaie, and J. Kleinberg, Proc. Natl. Acad. Sci. U.S.A. **115**, E11221 (2018).
[3] F. Musciotto, D. Papageorgiou, F. Battiston, and D. R. Farine bioRxiv (2022).
[4] A. Patania, G. Petri, and F. Vaccarino, EPJ Data Sci. **6**, 1 (2017).
[5] A. Zimmer, I. Katzir, E. Dekel, A. E. Mayo, and U. Alon, Proc. Natl. Acad. Sci. U.S.A. **113**, 10442 (2016).
[6] S. Klamt, U.-U. Haus, and F. Theis, PLoS Comput. Biol. **5**, e1000385 (2009).
[7] J. M. Levine, J. Bascompte, P. B. Adler, and S. Allesina, Nature (London) **546**, 56 (2017).
[8] G. Petri, P. Expert, F. Turkheimer, R. Carhart-Harris, D. Nutt, P. J. Hellyer, and F. Vaccarino, J. R. Soc. Interface **11**, 20140873 (2014).
[9] C. Giusti, R. Ghrist, and D. S. Bassett, J. Comput. Neurosci. **41**, 1 (2016).
[10] A. Santoro, F. Battiston, G. Petri, and E. Amico, Nat. Phys. **19**, 221 (2023).
[11] C. Berge, *Graphs and Hypergraphs* (North-Holland, Amsterdam, 1973).
[12] F. Battiston, G. Cencetti, I. Iacopini, V. Latora, M. Lucas, A. Patania, J.-G. Young, and G. Petri, Phys. Rep. **874**, 1 (2020).
[13] F. Battiston, E. Amico, A. Barrat, G. Bianconi, G. Ferraz de Arruda, B. Franceschiello, I. Iacopini, S. Kéfi, V. Latora, Y. Moreno *et al.*, Nat. Phys. **17**, 1093 (2021).
[14] M. T. Schaub, A. R. Benson, P. Horn, G. Lippner, and A. Jadbabaie, SIAM Rev. **62**, 353 (2020).
[15] T. Carletti, F. Battiston, G. Cencetti, and D. Fanelli, Phys. Rev. E **101**, 022308 (2020).
[16] C. Bick, P. Ashwin, and A. Rodrigues, Chaos **26**, 094814 (2016).
[17] P. S. Skardal and A. Arenas, Commun. Phys. **3**, 1 (2020).
[18] A. P. Millán, J. J. Torres, and G. Bianconi, Phys. Rev. Lett. **124**, 218301 (2020).
[19] M. Lucas, G. Cencetti, and F. Battiston, Phys. Rev. Res. **2**, 033410 (2020).
[20] L. V. Gambuzza, F. Di Patti, L. Gallo, S. Lepri, M. Romance, R. Criado, M. Frasca, V. Latora, and S. Boccaletti, Nat. Commun. **12**, 1 (2021).
[21] Y. Zhang, M. Lucas, and F. Battiston, Nat. Commun. **14**, 1605 (2023).
[22] I. Iacopini, G. Petri, A. Barrat, and V. Latora, Nat. Commun. **10**, 1 (2019).
[23] S. Chowdhary, A. Kumar, G. Cencetti, I. Iacopini, and F. Battiston, J. Phys. **2**, 035019 (2021).
[24] L. Neuhäuser, A. Mellor, and R. Lambiotte, Phys. Rev. E **101**, 032310 (2020).
[25] U. Alvarez-Rodriguez, F. Battiston, G. F. de Arruda, Y. Moreno, M. Perc, and V. Latora, Nat. Hum. Behav. **5**, 586 (2021).
[26] A. Civilini, N. Anbarci, and V. Latora, Phys. Rev. Lett. **127**, 268301 (2021).
[27] A. Civilini, O. Sadekar, F. Battiston, J. Gómez-Gardeñes, and V. Latora, arXiv:2303.11475.
[28] *Temporal Networks*, edited by P. Holme and J. Saramäki (Springer, Berlin, 2013).
[29] T. Takaguchi, N. Sato, K. Yano, and N. Masuda, New J. Phys. **14**, 093003 (2012).
[30] N. Perra, B. Gonçalves, R. Pastor-Satorras, and A. Vespignani, Sci. Rep. **2**, 1 (2012).

[31] A. Moinet, M. Starnini, and R. Pastor-Satorras, Phys. Rev. Lett. **114**, 108701 (2015).
[32] M. Karsai, M. Kivelä, R. K. Pan, K. Kaski, J. Kertész, A.-L. Barabási, and J. Saramäki, Phys. Rev. E **83**, 025102 (2011).
[33] I. Scholtes, N. Wider, R. Pfitzner, A. Garas, C. J. Tessone, and F. Schweitzer, Nat. Commun. **5** (2014).
[34] N. Masuda, K. Klemm, and V. M. Eguíluz, Phys. Rev. Lett. **111**, 188701 (2013).
[35] A. Moinet, M. Starnini, and R. Pastor-Satorras, New J. Phys. **21**, 093032 (2019).
[36] G. Cencetti, F. Battiston, B. Lepri, and M. Karsai, Sci. Rep. **11**, 1 (2021).
[37] L. Gallo, L. Lacasa, V. Latora, and F. Battiston, arXiv: 2303.09316.
[38] G. St-Onge, H. Sun, A. Allard, L. Hébert-Dufresne, and G. Bianconi, Phys. Rev. Lett. **127**, 158301 (2021).
[39] G. Petri and A. Barrat, Phys. Rev. Lett. **121**, 228301 (2018).
[40] M. Barthelemy, Phys. Rev. E **106**, 064310 (2022).
[41] O. T. Courtney and G. Bianconi, Phys. Rev. E **93**, 062311 (2016).
[42] J.-G. Young, G. Petri, F. Vaccarino, and A. Patania, Phys. Rev. E **96**, 032312 (2017).
[43] P. S. Chodrow, J. Complex Netw. **8**, cnaa018 (2020).
[44] K. Kovalenko, I. Sendiña-Nadal, N. Khalil, A. Dainiak, D. Musatov, A. M. Raigorodskii, K. Alfaro-Bittner, B. Barzel, and S. Boccaletti, Commun. Phys. **4**, 1 (2021).
[45] A. P. Millán, R. Ghorbanchian, N. Defenu, F. Battiston, and G. Bianconi, Phys. Rev. E **104**, 054302 (2021).
[46] M. Boguná and R. Pastor-Satorras, Phys. Rev. E **68**, 036112 (2003).
[47] R. Rastelli, N. Friel, and A. E. Raftery, Network Sci. **4**, 407 (2016).
[48] M. Kitsak, I. Voitalov, and D. Krioukov, Phys. Rev. Res. **2**, 043113 (2020).
[49] G. Caldarelli, A. Capocci, P. De Los Rios, and M. A. Munoz, Phys. Rev. Lett. **89**, 258702 (2002).
[50] K. Hoppe and G. J. Rodgers, Phys. Rev. E **90**, 012815 (2014).
[51] G. A. Miller, Y. Y. Shi, H. Qian, and K. Bomsztyk, Phys. Rev. E **75**, 051910 (2007).
[52] M. Boguná, R. Pastor-Satorras, A. Díaz-Guilera, and A. Arenas, Phys. Rev. E **70**, 056122 (2004).
[53] H. Hartle, F. Papadopoulos, and D. Krioukov, Phys. Rev. E **103**, 052307 (2021).
[54] M. Starnini and R. Pastor-Satorras, Phys. Rev. E **87**, 062807 (2013).
[55] M. Starnini and R. Pastor-Satorras, Phys. Rev. E **89**, 032807 (2014).
[56] See Supplemental Material at http://link.aps.org/supplemental/10.1103/PhysRevLett.132.037401 for detailed mathematical derivations.
[57] Q. F. Lotito, M. Contisciani, C. De Bacco, L. Di Gaetano, L. Gallo, A. Montresor, F. Musciotto, N. Ruggeri, and F. Battiston, J. Complex Netw. **11**, cnad019 (2023).
[58] A. V. Goltsev, S. N. Dorogovtsev, and J. F. F. Mendes, Phys. Rev. E **78**, 051105 (2008).
[59] M. Molloy and B. Reed, Random Struct. Algorithms **6**, 161 (1995).
[60] H. Sun and G. Bianconi, Phys. Rev. E **104**, 034306 (2021).